Clay–Polymer Nanocomposites Formed from Acidic Derivatives of Montmorillonite and an Epoxy Resin

Muh S. Wang and Thomas J. Pinnavaia*

Department of Chemistry and Center for Fundamental Materials Research, Michigan State University, East Lansing, Michigan 48824

A new type of clay–polymer nanocomposite has been prepared by the spontaneous self-polymerization of an epoxy resin, the diglycidyl ether of bisphenol A (DGEBA), and the concomitant delamination (exfoliation) of acidic forms of montmorillonite at elevated temperatures. The epoxide polymerization–clay delamination temperature (PDT) was dependent on the heating rate and the nature of the clay-exchange cation. H^+, NH_4^+, and acidic onium ions of the type $[H_3N(CH_2)_{n-1}COOH]^+$, $[H_3N(CH_2)_nNH_2]^+$, $[H_3N(CH_2)_nNH_3]^{2+}$, and $[H_3N(CH_2)_{n-1}CH_3]^+$ (n = 6 and 12) facilitated the polymerization–delamination process over the temperature range 198–287 °C. In general, the PDT increased with decreasing cation acidity and decreasing basal spacing of the clay. Evidence for nanocomposite formation was provided in part by a dramatic liquid-to-powder transformation of the clay–epoxide mixture upon formation of the polyether. The delamination of montmorillonite into 9.6-Å layers was further confirmed by transmission electron micrographs, which revealed interlayer separations up to $\sim$2000 Å and by the absence of clay reflections in the X-ray powder diffraction patterns. Differential scanning calorimetry studies of a polyether nanocomposite containing 5 wt % $[H_3N(CH_2)_{11}COOH]^+$–montmorillonite indicated the heat of reaction and activation energy for the organoclay-catalyzed polymerization reaction to be 228 and 108 kJ/mol, respectively.

Introduction

Smectite clays (e.g., montmorillonite) intercalated by polymeric molecules exhibit a wide range of novel physical properties.[1] One especially intriguing system recently reported by Toyota researchers[2] is based on the delamination (exfoliation) of $[H_3N(CH_2)_{11}COOH]^+$–montmorillonite in a semicrystalline nylon-6 matrix. The dispersion of the 9.6-Å-thin clay layers greatly improved the tensile strength (107 vs 69 MPa), tensile modulus (2.1 vs 1.1 Gpa), and heat distortion temperature (152 vs 65 °C) relative to pristine nylon-6. Also, replacing protonated 12-amino-lauric acid by protonated ε-caprolactam as the clay-exchange cation gave comparable improvements in composite tensile strength and modulus and increased the heat distortion temperature of nylon-6 to an even higher value (164 °C).[3]

Fujiwara and Sakamota[4] chose a very specific organo-clay–polymer system to demonstrate the swelling of the clay layers in a thermoplastic polyamide matrix. $[H_3N(CH_2)_5COOH]^+$–montmorillonite was dispersed in ε-caprolactam and the mixture was heated at 250 °C to form a clay/nylon-6 composite. The basal spacing of the organoclay in the nylon matrix was found to be 20 Å. Related experiments have been carried out using protonated 12-aminolauric acid $[H_3N(CH_2)_{11}COOH]^+$ as the

exchange cation.[5,6] The interlayer spacing was in the range 51–210 Å for organic montmorillonite loadings in the range 5–30 wt %. For protonated ε-caprolactam as the exchange cation,[3] the interlayer separation was found to be $\sim$250 Å.

It also has been reported in the patent literature[7] that dispersed montmorillonite particles (d_{001} = 50 Å) improved several mechanical properties of an amine-cured epoxy resin. $[H_3N(CH_2)_{11}COOH]^+$–montmorillonite enhanced the impact resistance (1.08 vs 0.91 J/m) and the heat distortion temperature (207 vs 193 °C) of epoxy resin Epicoat-828 cured by p,p'-diaminodiphenylsulfone (DDS). However, it was necessary to use N,N-dimethylformamide as a swelling solvent to achieve clay delamination in the polymer matrix.

Since epoxides are reactive toward self-polymerization to polyethers, it was of interest to us to investigate the direct polymerization of an epoxy resin in the galleries of montmorillonite in an effort to form clay–polyether nanocomposites. An especially important class of epoxy resin is the diglycidyl ether of bisphenol A (DGEBA) with the structure structure
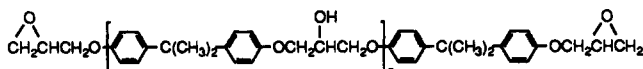
The commercially available resin, EPON-828 (Shell) with n = 0 (88%), n = 1 (10%), and n = 2 (2%)[8,9] and an average

® Abstract published in *Advance ACS Abstracts*, March 1, 1994.

(1) (a) Theng, B. K. G. *Formation and Properties of Clay–Polymer Complexes*; Elsevier: New York, 1979. (b) Giannelis, E. P. *JOM* **1992**, *44*, 28.

(2) (a) Okada, A.; Kawasumi, M.; Usuki, A.; Y. Kojima; Kuraurchi, T.; Kumigaito, O. *Mater. Res. Soc. Symp. Proc.* **1990**, *171*, 45. (b) Okada, A.; Kawasumi, M.; Kurauchi, T.; Kamigaito, O. *Polym. Prepr.* **1987**, *28*, 447.

(3) Kojima, Y.; Usuki, A.; Kawasumi, M.; Okada, A.; Kurauchi, T.; Kamigaito, O. *J. Polym. Sci., Part A: Polym. Chem.* **1993**, *31*, 983.

(4) Fujiwara, S.; Sakamota, T. Japan Patent 51 109,998, 1976.

(5) Fukushima, Y.; Okada, A.; Kawasumi, M.; Kurauchi, T.; Kamigaito, O. *Clay Miner.* **1988**, *23*, 27.

(6) Fukushima, Y.; Inagaki, S. *J. Inclus. Phenom.* **1987**, 473.

(7) Usuki, A.; Mizutani, T.; Fukushima, Y.; Fujimoto, M.; Fukumori, K.; Kojima, Y.; Sato, N.; Kurauchi, T.; Kamigaito, O. U.S. Patent 4,889,885, 1989.

(8) May, C. A., Ed. *Epoxy Resin*, 2nd ed.; Marcel Dekker: New York, 1988.

molecular weight of 378, was selected in the present work.

Experimental Section

Materials. Source clay SWy-1 (Wyoming Na⁺-montmorillonite) was obtained from the Clay Minerals Depository at the University of Missouri (Columbus, MO). Epoxy resin EPON-828 (Shell), aminocarboxylic acids $H_2N(CH_2)_{n-1}COOH$, primary diamines $H_2N(CH_2)_nNH_2$, and primary amines $CH_3(CH_2)_nNH_2$ (n = 6, and 12, Aldrich) were used as received.

Sample Preparation. The protonated forms of H_2N-$(CH_2)_{n-1}COOH$, $H_2N(CH_2)_nNH_2$, and $CH_3(CH_2)_nNH_2$ were formed by dissolving 10 mmol of the corresponding free amine in 1.0 L of a 0.01 N (0.02 N for $[H_3N(CH_2)_nNH_3]Cl_2$) HCl solution at 60 °C. Source clay SWy-1 (10 g or 7.64 mequiv) was thoroughly dispersed in the amine cation solution of interest at 60 °C for 3 h. The cation-exchanged montmorillonite was separated from the centrifugate and washed with deionized water. Centrifugation and washing were repeated until no white AgCl precipitate was observed when a drop of 0.1 N AgNO₃ was added to the centrifugate. The washed onium ion-exchanged montmorillonite was dispersed in 600 mL of deionized water and freeze-dried in a Labconco Freeze Dryer Model 18. The freeze-dried onium ion-montmorillonite was then sieved to <325 msh. Equivalent ion exchange reactions were used to prepare NH₄⁺- and H⁺-exchanged forms of the clay.

The desired amount of ion-exchanged clay was added to 15 g of epoxy resin EPON-828 and the clay-epoxide mixture was magnetically stirred in a 250-mL beaker at 75 °C for 30 min. The beaker was sealed with aluminum foil, and the temperature was then raised at a rate of ~20 °C/min to the clay delamination-epoxide polymerization temperature. The liquid-to-powder transformation of the mixture and the concomitant formation of the clay-epoxide nanocomposite took place within a period of 1 min.

Characterization. X-ray powder diffraction patterns were recorded by monitoring the diffraction angle 2θ from 2° to 45° on a Rigaku Rotaflex Ru-200BH X-ray diffractometer. The diffractometer was equipped with a Ni-filtered Cu Kα radiation source operated at 45 kV and 100 mA. The scanning speed and the step size used were 2°/min and 0.02°, respectively. Quartz was used as a calibration standard.

Clay-polymer nanocomposite samples for TEM studies were added to a Spurr's mixture in a silicon rubber mold, which was then placed in an oven at 70 °C overnight. The cured block was microtomed with a diamond knife and the resulting ultrathin sections (~90 nm) were mounted on a plastic-film support on a copper grid and examined with a JEOL 100CX transmission electron microscope operated at an accelerating voltage of 100 kV.

Clay-epoxide mixtures for DSC analyses (4.8-5.2 mg) were sealed hermetically in aluminum sample pans, and the DSC curves were recorded under N₂ (50 mL/min) on a duPont 910 differential scanning calorimeter at a heating rate of 20 °C/min. Indium (mp, 156.6 °C and ΔH_m, 28.42 J/g) was used for DSC calibration. In the case of the neat epoxy resin, the temperature was raised to 450 °C under the same experimental conditions, but the sample size was reduced to 2.5 mg to prevent pressure buildup and the rupture of the sealed sample pan.

TGA analyses were carried out under N₂ on a duPont 990 thermogravimetric analyzer using a heating rate of 20 °C/min.

Results and Discussion

The reaction of EPON-828 resin with H⁺-, NH₄⁺-, $[H_3N(CH_2)_{n-1}CH_3]^+$-, $[H_3N(CH_2)_{n-1}COOH]^+$-, $[H_3N$-$(CH_2)_nNH_2]^+$-, or $[H_3N(CH_2)_nNH_3]^{2+}$-exchanged forms of montmorillonite (where n = 6 and 12) at temperatures in the range 200-300 °C results in the polymerization of the epoxide and the concomitant delamination (exfoliation) of the clay structure. At the polymerization-
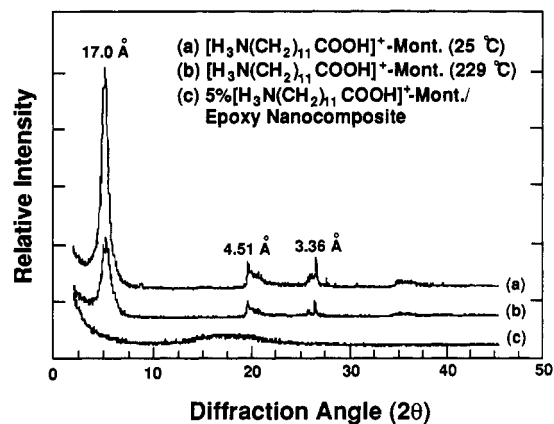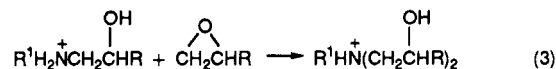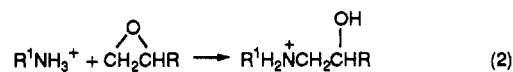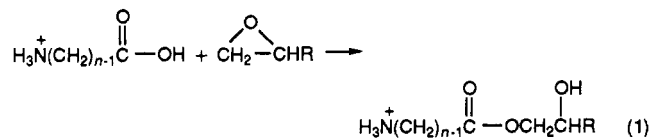
(9) Lee, H.; Neville, K. *Handbook of Epoxy Resins*; McGraw-Hill: New York, 1967.

Figure 1. XRD powder patterns for (a) freeze-dried $[H_3N(CH_2)_{11}$-COOH]⁺-montmorillonite, (b) $[H_3N(CH_2)_{11}COOH]^+$-montmorillonite freeze-dired and then heated at 229 °C, and (c) clay-polyether nanocomposite containing 5 wt % $[H_3N(CH_2)_{11}$-COOH]⁺-montmorillonite.

delamination temperature (PDT), which is dependent on the nature of the clay exchange cation, a dramatic liquid-to-powder transformation occurs which increases the bulk volume of the reaction mixture by a factor of 4-6. As will be shown below, the powdered products are novel polyether-clay nanocomposite materials.

Primary amines and carboxylic acids are commonly used as curing agents for epoxy resins owing to the reaction of amino and carboxylic groups with the epoxide ring according to eqs 1-3. However, at the onium ion clay

$$H_3\overset{+}{N}(CH_2)_{n-1}\overset{O}{\overset{\|}{C}}-OH + CH_2-CHR \longrightarrow$$

$$H_3\overset{+}{N}(CH_2)_{n-1}\overset{O}{\overset{\|}{C}}-OCH_2\overset{OH}{\overset{|}{C}}HR \qquad (1)$$

$$R^1NH_3^+ + CH_2-CHR \longrightarrow R^1H_2\overset{+}{N}CH_2\overset{OH}{\overset{|}{C}}HR \qquad (2)$$

$$R^1H_2\overset{+}{N}CH_2\overset{OH}{\overset{|}{C}}HR + CH_2-CHR \longrightarrow R^1H\overset{+}{N}(CH_2\overset{OH}{\overset{|}{C}}HR)_2 \qquad (3)$$

loadings used in the present work (typically, 5 wt %) the fraction of epoxide functional groups capable of reacting with the amino and carboxylic moieties on the clay-exchange cations is limited by stoichiometry to the range 1.4-2.8%. Thus, the protonated aminocarboxylic acid and primary diamine cations on the exchange sites of montmorillonite act primarily as acid catalysts rather than as curing agents. The acid catalytic role of the onium ions is verified by the fact that the same type of polymerization-delamination reaction is observed for the H⁺-, and NH₄⁺-, and $[H_3N(CH_2)_{n-1}CH_3]^+$-exchanged forms of the clay. Consequently, the primary polymerization reaction we are observing is the formation of a polyether according to eqs 4 and 5, where R'OH is an epoxy monomer possessing one or two hydroxyl groups.

$$RHC\overset{H\overset{+}{O}}{\overset{|}{C}}H_2 + RHC-CH_2 \longrightarrow RHC\overset{RHC}{\underset{H_2C}{\diagdown}}\overset{+}{O}-CHRCH_2OH \qquad (4)$$

$$RHC\overset{RHC}{\underset{H_2C}{\diagdown}}\overset{+}{O}-CHRCH_2OH + nRHC-CH_2 \longrightarrow$$

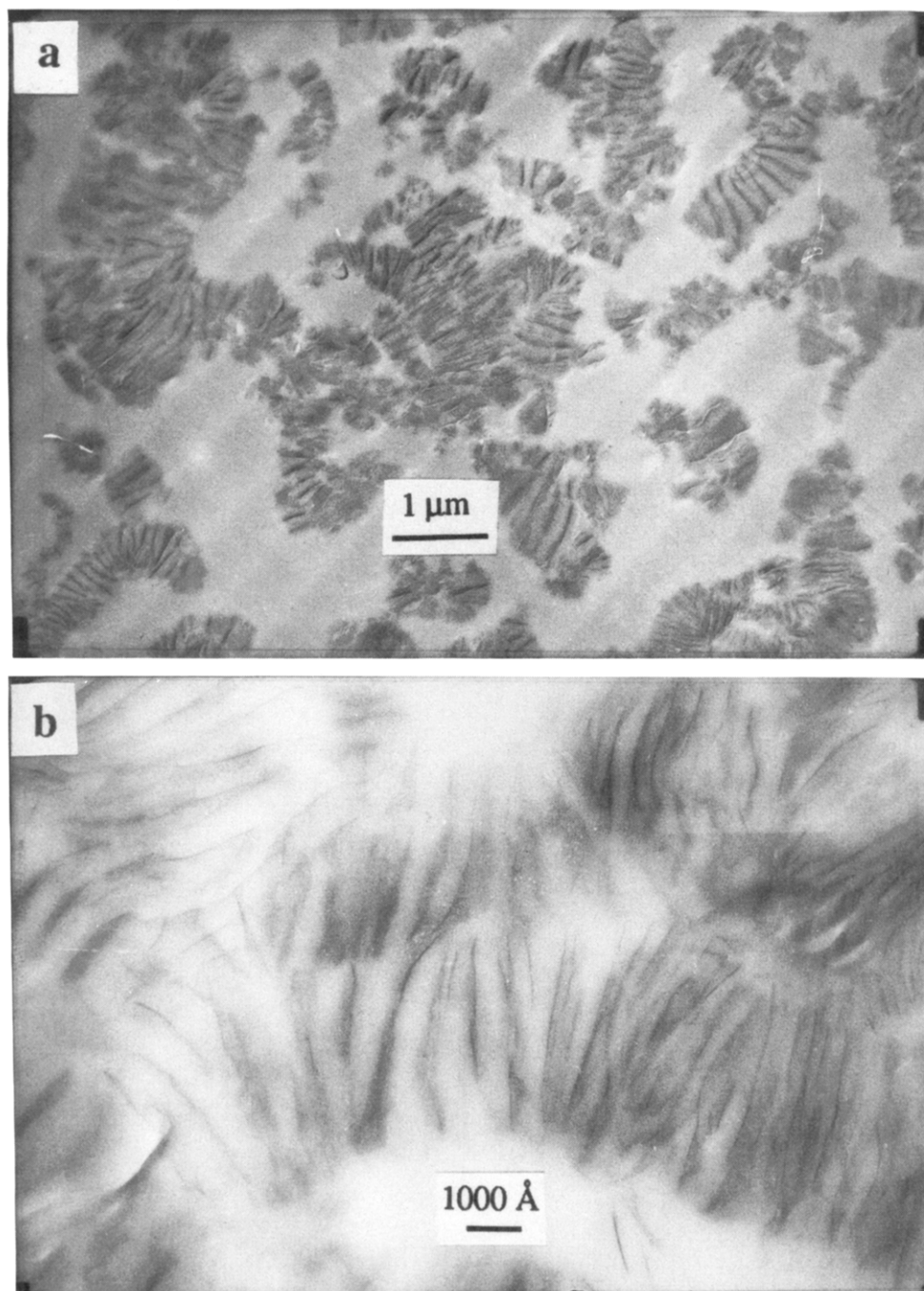$$RHC\overset{RHC}{\underset{H_2C}{\diagdown}}\overset{+}{O}-(CHRCH_2O)_nCHRCH_2OH \qquad (5)$$
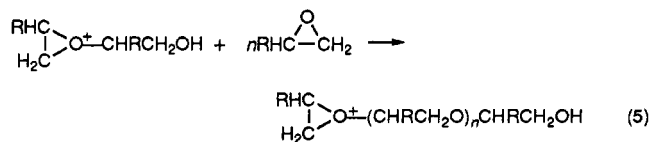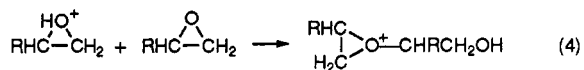
Figure 2. Transmission electron micrographs of a clay–polyether nanocomposite containing 5 wt % [H$_3$N(CH$_2$)$_{11}$-COOH]$^+$-montmorillonite: (a) ×10 000 and (b) ×58 000.

The delamination of the montmorillonite clay in the polymerized epoxy resin is confirmed by X-ray powder diffraction (XRD). As shown by the powder patterns in Figure 1a,b, [H$_3$N(CH$_2$)$_{11}$COOH]$^+$-montmorillonite remains crystalline over the temperature range 25–229 °C. However, no clay diffraction peaks are observed for a 5:95 (w/w) clay–polyether nanocomposite formed from [H$_3$N-(CH$_2$)$_{11}$COOH]$^+$-montmorillonite at 229 °C (Figure 1c). Only very diffuse scattering characteristic of the amorphous polyether appears in the XRD pattern of the composite. The absence of a 17.0-Å peak for [H$_3$N(CH$_2$)$_{11}$-COOH]$^+$-montmorillonite suggests that the clay particles (tactoids) have been exfoliated and the 9.6-Å-thick clay layers dispersed at the molecular level.

Transmission electron microscopy provides unambiguous evidence for the delamination of the clay in the polyether matrix. As shown in Figure 2, the TEM micrographs for a 5 wt % [H$_3$N(CH$_2$)$_{11}$COOH]$^+$-montmorillonite–polyether nanocomposite reveal that the micron-sized clay tactoids have been expanded by the polymer into accordian-like packets in which the interlayer spacings range up to 2000 Å. The shapes of the exfoliated particles reflect the initial stacking arrangement of layers in the tactoids. It is quite evident from the micrographs that epoxide monomers are polymerized in the gallery regions of the clay. Also, the clay-bound polyether becomes phase-segregated from the extragallery resin during the polymerization process. This phase segregation explains why a powdered morphology is realized for the nanocomposite rather than a monolithic structure. Related exfoliated tactoid morphologies were observed for the nanocomposites formed with the other acidic montmorillonites included in this work.

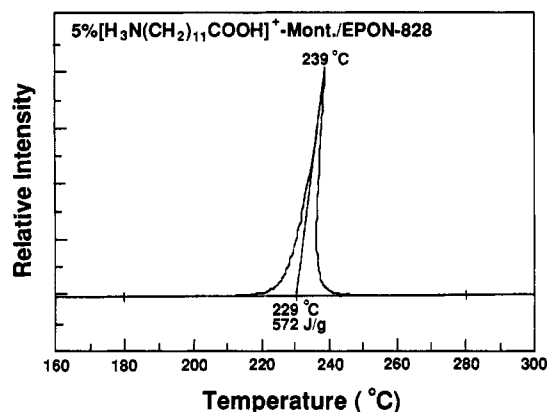The onset temperatures for polymerization–delamina-

Figure 3. Differential scanning calorimetry curve for the polymerization of Epon 828 epoxy resin in the presence of 5 wt % [H₃N(CH₂)₁₁COOH]⁺-montmorillonite at a heating rate of 20 °C/min.
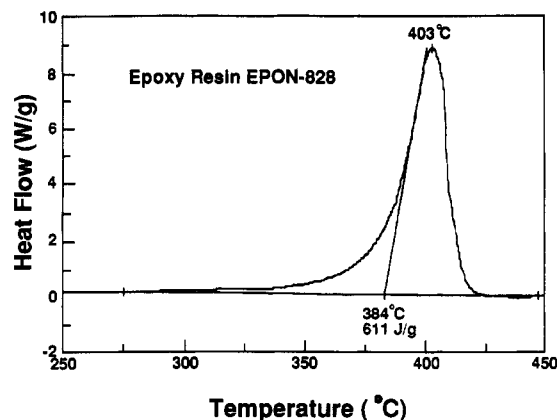

Figure 4. DSC thermogram (20 °C/min) for the uncatalyzed self-polymerization of epoxy resin EPON-828.
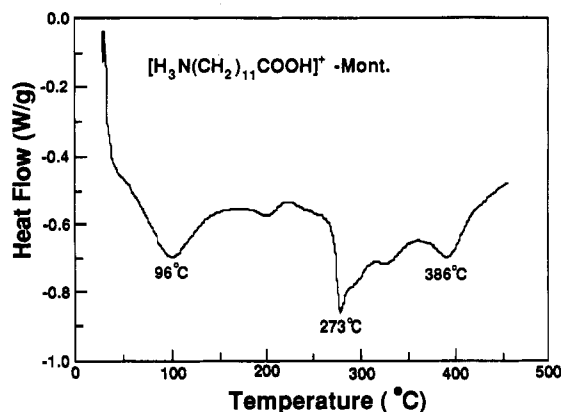

Figure 5. DSC thermogram (20 °C/min) for [H₃N(CH₂)₁₁-COOH]⁺-montmorillonite.

tion and the overall heats of reaction for nanocomposite formation were obtained by differential scanning calorimetry. Figure 3 shows the DSC curve for a 5:95 (w/w) mixture of [H₃N(CH₂)₁₁COOH]⁺-montmorillonite and epoxy resin EPON-828. The thermogram indicates that spontaneous clay exfoliation–epoxide polymerization process takes place at an onset temperature of 229 °C. On the basis of the integrated peak area, the heat of reaction is 572 J/g of composite. DSC curves for the neat epoxy resin and pristine [H₃N(CH₂)₁₁COOH]⁺-montmorillonite are shown for comparison purposes in Figures 4 and 5, respectively. In the absence of a catalyst self-polymerization of the neat resin occurs at a much higher onset
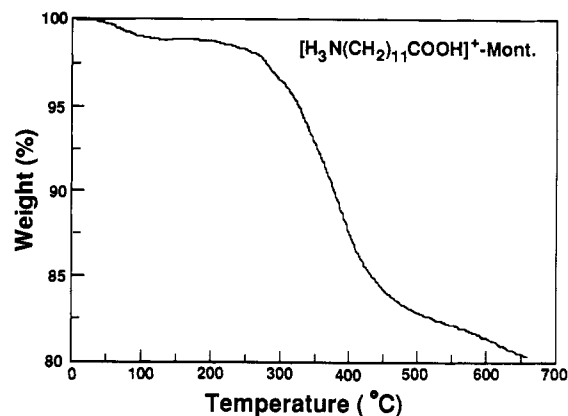
Figure 6. Thermogravimetric analysis curve (20 °C/min) for [H₃N(CH₂)₁₁COOH]⁺-montmorillonite.

Table 1. PDT Values and Thermodynamic Data for Clay–Polyether Nanocomposites Formed from Bifunctional Onium Ion Montmorillonites[a]

interlayer cation	initial basal spacing (Å)	PDT[b] (°C)	heat of reaction (J/g)	heat of polym[c] (kJ/mol)
[H₃N(CH₂)₁₁COOH]⁺	17.0 ± 0.1	229 ± 1	572 ± 16	228 ± 6
[H₃N(CH₂)₅COOH]⁺	13.3 ± 0.0	248 ± 1	565 ± 06	225 ± 2
[H₃N(CH₂)₁₂NH₃]²⁺	13.4 ± 0.1	271 ± 1	566 ± 08	225 ± 3
[H₃N(CH₂)₆NH₃]²⁺	13.1 ± 0.1	273 ± 2	568 ± 07	226 ± 3
[H₃N(CH₂)₁₂NH₂]⁺	13.5 ± 0.0	281 ± 2	563 ± 07	224 ± 3
[H₃N(CH₂)₆NH₂]⁺	13.2 ± 0.1	287 ± 2	557 ± 03	222 ± 2

[a] The clay:polymer composition was 5:95 (w/w). [b] PDT is the onset temperature for epoxide polymerization–clay delamination at a heating rate of 20 °C/min. [c] Heat of reaction for two epoxide equivalents.

temperature of 384 °C, but the heat of reaction (611 J/g) is comparable to that observed for the corresponding nanocomposite when corrected for the presence of clay (572/0.95 = 602 J/g). The DSC curve for the pure clay exhibits three weak endotherms near 96, 273, and 386 °C. These thermal features of the clay are too weak to observe for the 5 wt % nanocomposite. We assign the two endotherms below 300 °C to the loss of interparticle water (93 °C) and interlayer water (273 °C). Thermal decomposition of the intercalated onium ion most likely is responsible for the endotherm above 300 °C. The associated weight loss evident in the thermal gravimetric analysis curve shown in Figure 6 is compatible with this assignment. It is noteworthy that pure 12-aminolauric acid (mp, 186 °C) looses water of crystallization at 200–400 °C and thermally decomposes over the temperature range 400–500 °C, as judged by DSC and TGA analysis.

Listed in Table 1 are the onset polymerization–delamination temperatures (PDTs) and thermodynamic data for the polymerization of EPON-828 in the galleries of montmorillonite containing the bifunctional onium ions [H₃N(CH₂)ₙ₋₁COOH]⁺, [H₃N(CH₂)ₙNH₃]²⁺, and [H₃N-(CH₂)ₙNH₂]⁺ with n = 6 and 12. These exchanged forms of the clay exhibit basal spacings in the range 13.1–13.5 Å, except for the [H₃N(CH₂)₁₁COOH]⁺ derivative which has a spacing of 17.0 Å. Basal spacings of 13.3 Å (gallery height 3.7 Å) and 17.0 Å correspond to lateral monolayer and bilayer orientations for the onium ions, as illustrated schematically in Figure 7. Thus, the gallery surfaces of the 13.3-Å intercalates should be equally accessible to epoxide monomers on the basis of steric considerations. Although the average heat of polymerization (225 ± 2 kJ/mol resin) is independent of the bifunctional onium ion
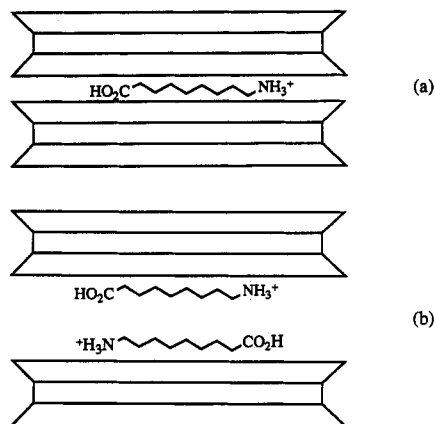
Figure 7. (a) Lateral monolayer and (b) lateral bilayer arrangements of gallery onium ions in montmorillonite.

Table 2. PDT Values and Thermodynamic Data for Clay-Polyether Nanocomposites Formed from Onium Ion, NH$_4$⁺, and H⁺ Montmorillonites

interlayer cation	basal spacing (Å)	PDT[a] (°C)	heat of reaction (J/g)	heat of polym[b] (kJmol)
[H$_3$N(CH$_2$)$_{11}$CH$_3$]⁺	15.9 ± 0.2	198 ± 1	550 ± 3	219 ± 2
[H$_3$N(CH$_2$)$_5$CH$_3$]⁺	14.9 ± 0.1	287 ± 1	554 ± 6	220 ± 3
NH$_4$⁺	12.5 ± 0.1	247 ± 1	554 ± 5	220 ± 2
H⁺	13.9 ± 0.1	231 ± 1	555 ± 12	221 ± 5

[a] The PDT is the onset temperature for epoxide polymerization-clay delamination at a heating rate of 20 °C/min and a composite a clay:polymer composition of 5:95 (w/w). [b] Heat of polymerization for two epoxide equivalents.

and equivalent on the heats typically observed for amine-cured epoxy resins,[8,9] the PDTs are quite sensitive to the structure of the onium ion. Being best correlated with the intrinsic acidity of the ion, the PDT values for the bifunctional onium ion clays decrease in the order [H$_3$N(CH$_2$)$_{n-1}$COOH]⁺ (n = 6) < [H$_3$N(CH$_2$)$_n$NH$_3$]²⁺ < [H$_3$N(CH$_2$)$_n$NH$_2$]⁺ (n = 6, 12). The lowest PDT in this series (229 °C) is observed for [H$_3$N(CH$_2$)$_{11}$COOH]⁺ montmorillonite. In this latter case the basal spacing (17.0 Å) corresponds to a lateral bilayer structure, which should make the galleries more accessible to epoxide monomers.

Table 2 summarizes the PDT and thermodynamic values for epoxide polymerization in the galleries of [H$_3$N-(CH$_2$)$_{n-1}$CH$_3$]⁺ (n = 6 and 12), NH$_4$⁺, and H⁺ montmorillonites. As expected, the heats of polymerization are independent of the clay exchange cation within experimental error, but the PDTs are very cation dependent. Figure 8 compares the DSC exotherms for the most reactive and least reactive clays studied in the present work, namely, [H$_3$N(CH$_2$)$_{11}$CH$_3$]⁺- and [H$_3$N(CH$_2$)$_5$CH$_3$]⁺-montmorillonite with PDT values of 198 and 287 °C, respectively. It is noteworthy that the most acidic clay, H⁺-montmorillonite, exhibits a PDT (231 °C) intermediate between the least reactive and most reactive onium ion clay systems. This latter result also indicates that interlayer *accessibility*, as well as gallery cation acidity, is important in determining reactivity toward nanocomposite formation.

The dependence of PDT on clay concentration has been investigated for [H$_3$N(CH$_2$)$_{11}$COOH]⁺- and [H$_3$N(CH$_2$)$_5$-COOH]⁺-montmorillonites. Figure 9 shows that the PDT rapidly decreases at loadings below 1.0 wt % and levels off as the clay concentration is increased above 2.0 wt %. That is, only a very small organoclay concentration is needed to effectively catalyze the epoxide polymerization-clay delamination process. For instance, the uncatalyzed
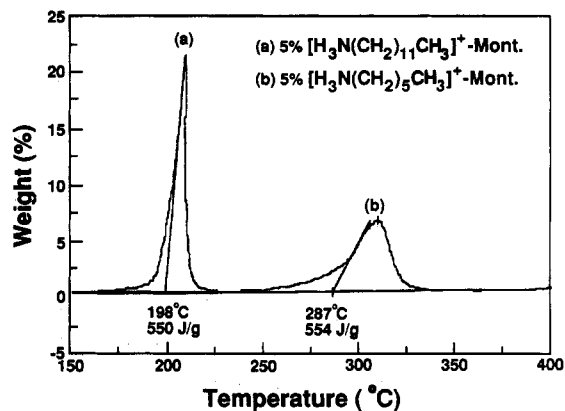

Figure 8. Comparison of DSC curves for epoxide polymerization in the presence of 5 wt % (a) [H$_3$N(CH$_2$)$_{11}$CH$_3$]⁺- and (b) [H$_3$N(CH$_2$)$_5$CH$_3$]⁺-montmorillonites. The heating rate was 20 °C/min.

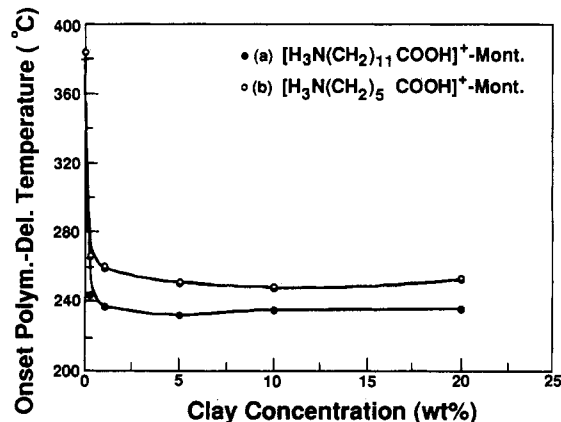**Figure 9.** Dependence of onset temperature for epoxide polymerization-clay delamination on clay concentration: (●) [H$_3$N(CH$_2$)$_{11}$COOH]⁺ montmorillonite; (O) [H$_3$N(CH$_2$)$_5$COOH]⁺ montmorillonite.
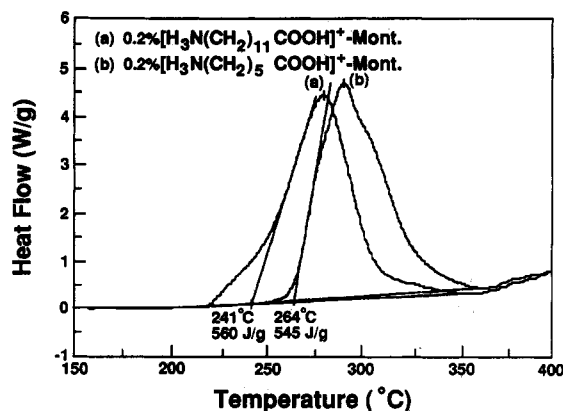
Figure 10. DSC thermograms (20 °C/min) for Epon 828 polymerization catalyzed by 0.2 wt % (a) [H$_3$N(CH$_2$)$_{11}$COOH]⁺- and (b) [H$_3$N(CH$_2$)$_5$COOH]⁺-montmorillonites.

epoxide self-polymerization temperature is 384 °C, compared to 241 and 264 °C for epoxide polymerizations catalyzed by 0.2 wt % [H$_3$N(CH$_2$)$_{11}$COOH]⁺- and [H$_3$N(CH$_2$)$_5$COOH]⁺-montmorillonites, respectively. However, as indicated by the broadness of the DSC curves in Figure 10, the clay-catalyzed epoxide polymerizations are relatively sluggish. Also, the relatively small values for the heat of reaction (560 and 545 J/g) indicate that polyether formation is incomplete at low clay concentrations. On the basis of the extrapolated heat of reaction (see below), the extent of epoxide polymerization is
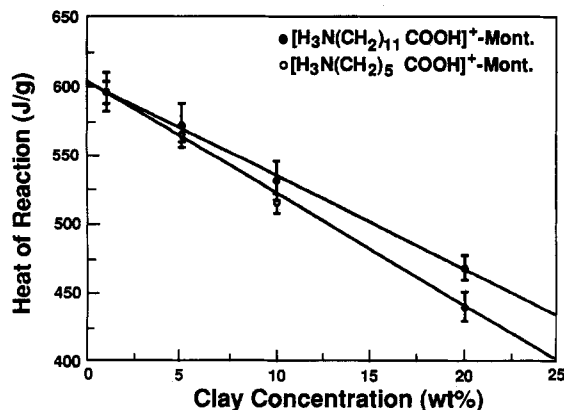
Clay–Polymer Nanocomposites

Chem. Mater., Vol. 6, No. 4, 1994 **473**

Figure 11. Heat of reaction for clay–polyether nanocomposite formation as a function of the clay concentration for (●) [H$_3$N(CH$_2$)$_{11}$COOH]$^+$– and (○) [H$_3$N(CH$_2$)$_5$COOH]$^+$–montmorillonites.

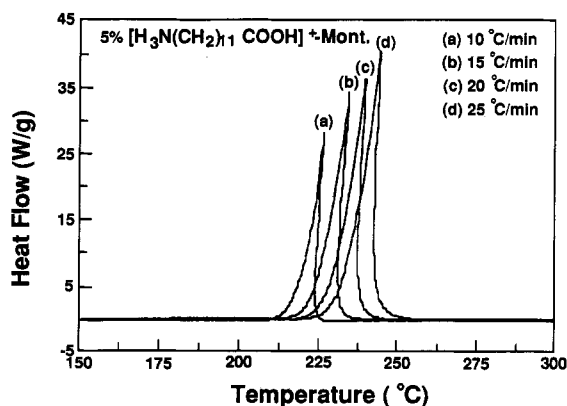**Figure 12.** DSC thermograms for epoxide polymerization catalyzed by 5 wt % [H$_3$N(CH$_2$)$_{11}$COOH]$^+$–montmorillonite at heating rates of: 10, 15, 20, and 25 °C/min.

estimated to be 94 and 91% for reactions catalyzed by 0.2 wt % [H$_3$N(CH$_2$)$_{11}$COOH]$^+$– and [H$_3$N(CH$_2$)$_5$COOH]$^+$– montmorillonites, respectively. Thus, clay loadings of at least 2.0 wt % are need to achieve optimal nanocomposite formation.

In Figure 11 the heat of reaction is plotted against the clay concentration for [H$_3$N(CH$_2$)$_{11}$COOH]$^+$– and [H$_3$N-(CH$_2$)$_5$COOH]$^+$–montmorillonite. For each system the heat of reaction decreases linearly with increasing clay concentration. The extrapolated values are 603 and 604 J/g or 228 kJ/mol of neat epoxide. The linear relationship again shows that the heat of reaction is due primarily to epoxide polymerization. The greater slope for [H$_3$N(CH$_2$)$_5$-COOH]$^+$ montmorillonite suggests that the polymerization is somewhat less complete, especially at high clay concentrations, relative to [H$_3$N(CH$_2$)$_{11}$COOH]$^+$–montmorillonite. The ratio of the heat of reaction for [H$_3$N(CH$_2$)$_5$-COOH]$^+$–montmorillonite to that for [H$_3$N(CH$_2$)$_{11}$-COOH]$^+$–montmorillonite is 0.94 at a clay concentration of 20 wt %. This may indicate that the gallery region is more accessible for reaction when the longer chain aminoacid cataion occupies the clay exchange sites.

To obtain activation energies for a typical clay–polyether nanocomposite system, the temperature dependence of epoxide polymerization in the galleries of 5 wt % [H$_3$N(CH$_2$)$_{n-1}$COOH]$^+$ (n = 6, 12) montmorillonites was determined by DSC. Plots of the DSC curves at various heating rates (e.g., 10–25 °C/min) are shown in Figure 12 for the [H$_3$N(CH$_2$)$_{11}$COOH]$^+$ montmorillonite–EPON-828

Table 3. Kinetics Parameters for Clay–Polyether Nanocomposites Formed from [H$_3$N(CH$_2$)$_{n-1}$COOH]$^+$– (n = 6, 12) Montmorillonites

interlayer cation	PDT^a (°C)	E_a (kJ/mol)	A (s^{-1})	$\Delta S^{\circ\ast c}$ (eu)
[H$_3$N(CH$_2$)$_5$COOH]$^+$	248 ± 1	105 ± 1	3.06 × 10^8	−24.8 ± 0.1
[H$_3$N(CH$_2$)$_{11}$COOH]$^+$	229 ± 1	108 ± 1	1.80 × 10^9	−21.2 ● 0.1

^{a} Polymerization–delamination temperature determined at a heating rate of 20 °C/min and a clay loading of 5.0 wt %. ^{a} Activation entropy calculated at the PDT.

system. These curves show that the peak maximum temperature (T_p) increases with increasing heating rate (φ). The following emperically derived equation[10-13] relating T_p and φ can be used to evaluate the activation energy (E_a), regardless of the reaction order:

$$\frac{d \ln \varphi}{d(1/T_p)} \approx -\frac{1.052 E_a}{R} \qquad (6)$$

The preexponential or frequency factors (A) for the polymerization reactions can be obtained from the following expression:[10,11,14]

$$A \approx \frac{\varphi E_a \exp(E_a/RT_p)}{RT_p^2} \qquad (7)$$

Also, the relationship between the preexponential factor and the activation entropy in the standard state ($\Delta S^{\circ\ast}$) is given by

$$\Delta S^{\circ\ast} = R \ln \frac{Ah(c^\circ)^{m-1}}{kTe^m} \qquad (8)$$

where m is the molecularity of an elementary reaction or the number of molecules that come together to form the activated complex; $(c^\circ)^{m-1}$ is the factor required to keep the equilibrium constant ($K^\ast$) dimensionless; and h and k are the Planck and Boltzman constants, respectively. For bimolecular acid-catalyzed epoxide ring openings, m = 2.

Table 3 summarizes the activation parameters for the formation of clay–polyether nanocomposites from [H$_3$N-(CH$_2$)$_5$COOH]$^+$ and [H$_3$N(CH$_2$)$_{11}$COOH]$^+$ montmorillonite. The activation energies for these two systems namely, 105 and 108 ± 2 kJ/mol, respectively, are identical within experimental error. These values compare with reported activation energies of 75–88 kJ/mol for related epoxide polymerizations.[15-17] The higher values obtained for our nanocomposite systems might be due to an increase in steric hindrance caused by the intercalation of the growing polymer chain between clay layers. Clearly, the differences in the reactivities of the two onium ion montomorillonites arises primarily from differences in activation entropy. The entropy is substantially more negative for [H$_3$N(CH$_2$)$_5$-COOH]$^+$–montmorrilonite, suggesting that the galleries

(9) Kissinger, H. E. *Anal. Chem.* **1957**, *29*, 1702.
(10) Prime, R. B. *Thermal Characterization of Polymeric Materials*; Turi, E., Ed.; Academic: New York, 1981.
(11) Ozawa, T. *J. Therm. Anal.* **1970**, *2*, 301.
(12) Doyle, C. D. *Anal. Chem.* **1951**, *33*, 79.
(13) Prime, R. B. *Polym. Eng. Sci.* **1973**, *13*, 365.
(14) Peyer, P.; Bascom, W. D. *J. Polym. Sci., Polym. Phys. Ed.* **1975**, *18*, 129.
(15) Swarim, S. J.; Wims, A. M. *Anal. Calorim.* **1976**, *4*, 155.
(16) Cizemciogly, M.; Gupta, A. *SAMPLE Q.* **1982**, *April*, 16.

are more ordered and, hence, less accessible than in $[H_3N(CH_2)_{11}COOH]^+$ montmorillonite.

Conclusions

In this work we have achieved the direct nanoscopic delamination of acidic smectite clays in a polyether matrix derived from the polymerization of an epoxy resin. The exfoliation of the clay layers takes place spontaneously at the delamination–polymerization temperature. In addition to simple acidic cations such as H^+ and NH_4^+, various onium ions, namely, protonated primary amines, diamines, and aminocarboxylic acids, are suitable delaminating agents.

The delamination–polymerization temperature depends on the heating rate and the nature of the clay-exchange cation. The heating rate being equal, cation acidity and interlayer accessability are the two most important factors affecting the delamination-polymerization temperature. Within experimental error, the heat of epoxide polymerization is independent of the cation-exchange form of montmorillonite, suggesting that differences in the clay exfoliation energy are small relative to the epoxide polymerization energy. The activation entropy, as reflected in the preexponential factor, is important in determining differences in the reactivities of organoclay–epoxide systems.

Owing to their powdery texture, the clay–polymer nanocomposites of the present work are not suitable for mechanical measurements. Powder formation is caused by phase segregation of the clay-bound polyether and the epoxy resin. It should be possible, however, to circumvent this limitation using more compatible cyclic ethers as polymer precursors. Also, powder processing methods may offer a convenient route to the formation of monolithic structures.